Metasurface hologram for polarization measurement

Optics Letters

Metasurface hologram for polarization measurement

Scott Hermon,[1,†] Aning Ma,[1,2,†] Fuyong Yue,[1] Fillmon Kubrom,[1] Yuttana Intaravanne,[1] Jin Han,[3] Yong Ma,[4] and Xianzhong Chen[1,*]

[1]Institute of Photonics and Quantum Sciences, School of Engineering and Physical Sciences, Heriot-Watt University, Edinburgh EH14 4AS, UK
[2]School of Information Science and Engineering, Lanzhou University, Lanzhou 730000, China
[3]College of Materials Science and Engineering, Kunming University of Science and Technology, Kunming 650093, China
[4]School of Optoelectronic Engineering, Chongqing University of Posts and Telecommunications, Chongqing 400065, China
*Corresponding author: x.chen@hw.ac.uk

Received 16 May 2019; revised 3 July 2019; accepted 12 July 2019; posted 15 July 2019 (Doc. ID 367798); published 4 September 2019

Polarization measurement is crucial for many optical applications in science and technology. Geometric metasurfaces have been used to develop polarization-sensitive holograms, providing a new opportunity for polarization measurement. We propose and experimentally demonstrate a hologram method to measure the polarization state of light. A reflective-type metasurface hologram is used to generate holographic images of graphene pattern. The ellipticity and helicity of the incident light are measured based on the intensities of the neighboring light spots, corresponding to two opposite circular polarization states. Benefiting from the advantages of reflective geometric metasurfaces, this device can operate in broadband.

https://doi.org/10.1364/OL.44.004436

Polarization is a fundamental property of electromagnetic radiation; this property specifies the orientation in which a wave oscillates. A light beam can be polarized into different polarization states such as linear, elliptical, and circular polarization states. These states of polarization are mainly determined by two parameters: the handedness and the ellipticity. A typical method to measure these parameters is based on an optical system consisting of many optical devices such as polarizers, waveplates, and polarization modulators. By measuring the flux as light passes through them, the appropriate calculations can be made to determine the polarization state. However, these optical devices are often very bulky, limiting their applications in system integration. Furthermore, although the polarization state can be measured, the approach is not elegant and efficient.

Metasurfaces are two-dimensional (2D) counterparts of metamaterials, which can manipulate light propagation in a desirable manner, providing an unusual approach to realizing a plethora of metasurface devices with unusual functionalities, including lenses [1–6], couplers [7–9], holograms [10–12], invisibility cloaking [13–15], arbitrary polarization manipulation [16,17], nonlinear metasurfaces [18,19], and fluorescence emission control [20]. Various types of metasurface devices for polarization measurement have been demonstrated [21–23]. However, an approach based on polarization-sensitive metasurface hologram has not been reported.

In this Letter, we propose and experimentally demonstrate a hologram approach for measuring the polarization state of a light beam. Figure 1 shows the schematic of our proposed approach, which is based on the reconstructed holographic images upon the illumination of the light beam. When the light beam with pure left circular polarization (LCP) is incident on the metasurface, a clear holographic image (graphene pattern) is seen. A holographic image of the same graphene pattern with a rotated angle is observed, when the polarization state of the light is changed from LCP to right circular polarization (RCP). The two holographic images overlap upon the illumination of the light beam with linear polarization (LP), since it can be decomposed into LCP beam and RCP beam with equal components. For a light beam with elliptical polarization, the intensities of the two holographic images for LCP and RCP are different, because the two components for LCP and RCP beams are different. Due to the unique pattern of the graphene structures, the polarization state of the incident light can be determined by measuring the intensities of the two neighboring light spots in the overlap area of holographic images.

Our system shown in Fig. 1 consists of five main parts: the laser, the polarizer, the quarter-wave plate, the metasurface, and the screen. The metasurface is illuminated by the light from the laser, which is polarized as it passes through the linear polarizer and then the quarter-wave plate before impinging on the metasurface hologram. The holographic image is reconstructed on the screen by the light reflected from the metasurface. To generate the polarization-sensitive metasurface hologram for polarization measurement, two graphene patterns [Fig. 2(a)] are encoded in the metasurface upon the illumination of LCP light. The center-to-center distance between these two patterns is $2z_0$. The pattern on the right is the same as that on the left, but it is rotated at an angle of 11°, which can ensure that there are some separated neighboring light spots in the overlapped

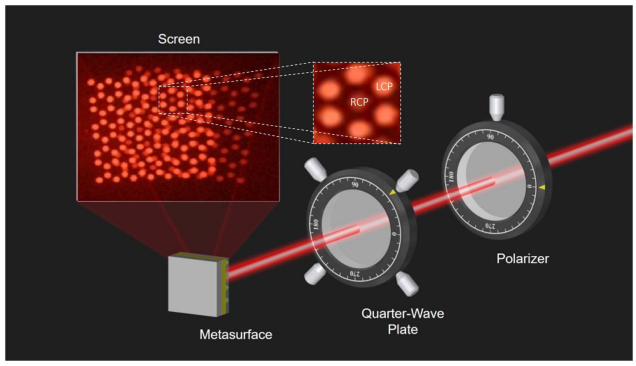

Fig. 1. Three-dimensional schematic of the experimental set-up to demonstrate the polarization measurement based on the reconstructed holographic images. LCP, Left circular polarization; RCP, right circular polarization.

area. The off-axis angle of the reflected images on both sides is 30 deg. The size of the holographic image is proportional to the distance between the sample and screen, but the overlap of the two patterns is not affected. The Gerchberg–Saxton algorithm is used to retrieve the required phase profile. The reflective-type metasurface consisting of metallic nanorods with spatially variant orientation and ground metallic film with the dielectric layer sandwiched between them is used to generate Pancharatnam–Berry phase over a broad range of wavelengths with high efficiency. More details about diffraction efficiency and bandwidth are available in Ref. [24]. 32-phase levels of phase distribution are used to minimize the near-field coupling between neighboring nanorods. A metasurface hologram with a pixel size of 300 nm × 300 nm and pixel number of 2000 × 2000 is designed to improve the fidelity of the constructed image. The scanning electron microscope (SEM) image of the fabricated metasurface consisting of nanorods with spatially varying orientation is shown in Fig. 2(b). The nanorods all have identical geometric parameters. They have a width of 50 nm and a length of 200 nm, along with a thickness of 40 nm. A 150 nm thick gold film and an 85 nm thick glass spacer are deposited on the silicon substrate by electron beam evaporation. The whole size of the sample is 600 μm × 600 μm. The design and fabrication details are available in Ref. [25]. The three-layer structure functions like a Fabry–Perot–like cavity, where the thickness of the SiO_2 spacer corresponds to the cavity length. The nanorod, along with the spacer and the background layer, functions as a reflective-type half-wave plate.

To experimentally demonstrate the hologram polarization state measurement approach, various polarization states of incident light are analyzed by measuring the intensities of specific light spots of the two holographic images. These two light spots are chosen so that there is no overlap between the two images; otherwise, it would be impossible to distinguish between the intensities of the two images. To measure the intensity, a software called ImageJ is used. The polarization state of the incident light could be varied by the use of a quarter-wave plate and a linear polarizer placed in front of a laser source. While the fast axis of the quarter-wave plate is fixed, the orientation of the transmission axis of the linear polarizer is rotated, so that the polarization state of the incident light will change depending on the angle between the two axes. The angle between the polarizer and quarter-wave plate is initially set to be 45°; then it is rotated in steps of 5°. The metasurface is mounted on a 2D translational stage, and a white screen is used to observe the reconstructed images.

Based on the experiment above, Fig. 3(a) shows five different holographic images (graphene patterns) upon the illumination of the light beam with a wavelength of 633 nm. When the incident light is pure LCP, the intensity of the right image (I_{RCP}) is negligible. Upon illumination with the left-hand elliptical polarized light, the intensities of the left image (I_{LCP}) are larger than that of I_{RCP}. Similarly, the intensity relation for the right-hand elliptical light ($I_{RCP} > I_{LCP}$) and the pure RCP ($I_{LCP} \approx 0$) can be obtained. When the polarization state of the incident light is linear polarization (LP), which consists of equal RCP and LCP components, the intensities of the two images ($I_{RCP} = I_{LCP}$) are equal. Therefore, the handedness and ellipticity of the incident light can be determined through comparing the intensity of LCP and RCP from the holographic images. As seen from Fig. 3(a), the metasurface clearly demonstrates the brightness of the two constructed holographic images closely depends on the polarization state of the incident light.

To further confirm the feasibility of our proposed approach, the normalized intensity data are plotted, as seen in Fig. 3(b). It can be seen from the fits that as the intensity of the RCP light spot decreases, the intensity of the LCP light spot increases. The polarization state of the light can be represented by a point

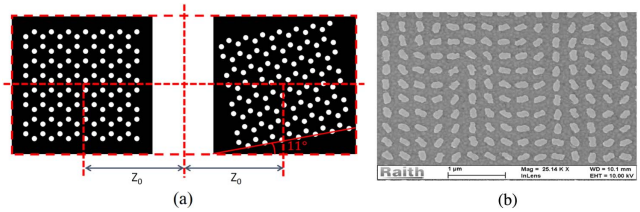

Fig. 2. (a) Computer-generated hologram graphene pattern. The center-to-center distance between these two patterns is $2z_0$. The pattern on the right is the same as that on the left, but it is rotated at an angle of 11°. (b) SEM image of the fabricated metasurface, which consists of three layers: gold nanorods with spatially variant orientations on the top, gold film at the bottom, and the silicon dioxide layer sandwiched between them.

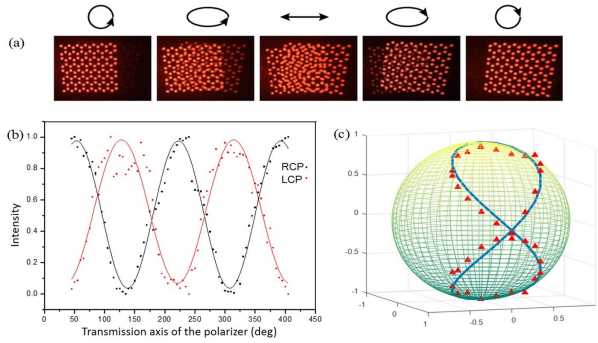

Fig. 3. (a) Five different holographic images of the graphene pattern; the polarization states of light from left to right are LCP, left elliptical polarization, LP, right elliptical polarization, and RCP. (b) Normalized intensity measurements of RCP and LCP light. (c) Experimental (rod triangles) and theoretical data (solid line) on a Poincaré sphere.

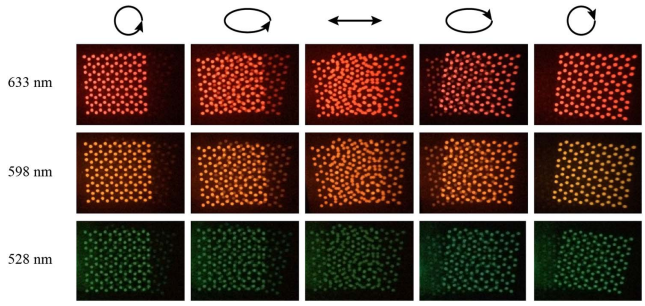

Fig. 4. Holographic images of graphene patterns for the incident polarization states at the wavelengths of 633, 598, and 528 nm.

on a Poincaré sphere. The experimental and theoretical data are plotted against each other on the Poincaré sphere [see Fig. 3(c)]. The ellipticity η and helicity of the incident light can be calculated by the intensity ratio $\tau = I_{\mathrm{LCP}}/I_{\mathrm{RCP}}$, $\eta = (1 - \sqrt{\tau})/(1 + \sqrt{\tau})$. $\eta = \pm 1$ and $\eta = 0$ correspond to RCP (LCP) and LP, respectively. The detailed information is available in Ref. [16]. As we can see from the plot, the experimental data (little red triangle) and theoretical data (blue line) agree well. Benefiting from the exotic property of reflective-type metasurface, the metasurface hologram can work in broadband. The holographic images for a range of incident polarization states at 633, 598, and 528 nm are given in Fig. 4, respectively. The figures in Figs. 3(a) and 4 are only half of the image window from Fig. 2(a), and the efficiency on one side is halved. This approach provides a fast way to roughly estimate the polarization state of the incident based on the intensity difference between two holographic images. Although the approach can be used to measure the ellipticity of the polarized light, the full polarization measurement also needs further information (e.g., the polarization azimuth angle discussed in the Refs. [26,27]).

In conclusion, a metasurface hologram approach for polarization measurement is experimentally demonstrated. The ellipticity and helicity of various polarizations states of the incident light are measured based on intensities of the neighboring light spots from the reconstructed images. The dynamic polarization change of a light beam can be quickly estimated based on the rise and fall of intensities of the reconstructed holographic images, providing a fast and elegant polarization measurement method based on polarization-sensitive metasurface holograms.

Funding. Engineering and Physical Sciences Research Council (EP/P029892/1); Natural Science Foundation of Gansu Province (17JR5RA197); China Scholarship Council (201808535073); Chongqing Research Program of Basic Research and Frontier Technology (cstc2016jcyA0301); Venture & Innovation Support Program for Chongqing Overseas Returnees and key program (A2018-01).

[†]These authors contributed equally to this Letter.

REFERENCES

1. L. Verslegers, P. B. Catrysse, Z. F. Yu, J. S. White, E. S. Barnard, M. L. Brongersma, and S. H. Fan, Nano Lett. **9**, 235 (2009).
2. X. Z. Chen, L. L. Huang, H. Mühlenbernd, G. X. Li, B. F. Bai, Q. F. Tan, G. F. Jin, C. W. Qiu, S. Zhang, and T. Zentgraf, Nat. Commun. **3**, 1198 (2012).
3. A. Pors, M. G. Nielsen, R. L. Eriksen, and S. I. Bozhevolnyi, Nano Lett. **13**, 829 (2013).
4. X. Wan, W. X. Jiang, H. F. Ma, and T. J. Cui, Appl. Phys. Lett. **104**, 151601 (2014).
5. J. T. Hu, C. H. Liu, X. C. Ren, L. J. Lauhon, and T. W. Odom, ACS Nano. **10**, 10275 (2016).
6. X. H. Yin, T. Steinle, L. L. Huang, T. Taubner, M. Wuttig, T. Zentgraf, and H. Giessen, Light Sci. Appl. **6**, e17016 (2017).
7. J. Lin, J. P. Balthasar Mueller, Q. Wang, G. H. Yuan, N. Antoniou, X. C. Yuan, and F. Capasso, Science **340**, 331 (2013).
8. A. Baron, E. Devaux, J. C. Rodier, J. P. Hugonin, E. Rousseau, C. Genet, T. W. Ebbesen, and P. Lalanne, Nano. Lett. **11**, 4207 (2011).
9. S. L. Sun, Q. He, S. Y. Xiao, Q. Xu, X. Li, and L. Zhou, Nat. Mater. **11**, 426 (2012).
10. G. X. Zheng, H. Mühlenbernd, M. Kenney, G. X. Li, T. Zentgraf, and S. Zhang, Nat. Nanotechnol. **10**, 308 (2015).
11. W. M. Ye, F. Zeuner, X. Li, B. Reineke, S. He, C. W. Qiu, J. Liu, Y. T. Wang, T. Zentgraf, and S. Zhang, Nat. Commun. **7**, 11930 (2016).
12. X. Li, L. W. Chen, Y. Li, X. H. Zhang, M. B. Pu, Z. Y. Zhao, X. L. Ma, Y. Q. Wang, M. H. Hong, and X. G. Luo, Sci. Adv. **2**, e1601102 (2016).
13. L. Y. Hsu, T. Lepetit, and B. Kanté, Prog. Electromagn. Res. **152**, 33 (2015).
14. H. C. Chu, Q. Li, B. B. Liu, J. Luo, S. L. Sun, Z. H. Hang, L. Zhou, and Y. Lai, Light Sci. Appl. **7**, 50 (2018).
15. W. Zhao, H. C. Chu, Z. Tao, and Z. H. Hang, Appl. Phys. Express **12**, 054004 (2019).
16. D. D. Wen, F. Y. Yue, S. Kumar, Y. Ma, M. Chen, X. M. Ren, P. E. Kremer, B. D. Gerardot, M. R. Taghizadeh, G. S. Buller, and X. Z. Chen, Opt. Express **23**, 010272 (2015).
17. P. Yu, S. Q. Chen, J. X. Li, H. Cheng, Z. C. Li, W. W. Liu, B. Y. Xie, Z. C. Liu, and J. G. Tian, Opt. Lett. **40**, 3229 (2015).
18. G. X. Li, S. Zhang, and T. Zentgraf, Nat. Rev. Mater. **2**, 17010 (2017).
19. A. Krasnok, M. Tymchenko, and A. Alù, Mater. Today **21**(1), 8 (2018).
20. S. Luo, Q. Li, Y. Q. Yang, X. X. Chen, W. Wang, Y. R. Qu, and M. Qiu, Laser Photonics Rev. **11**, 1600299 (2017).
21. A. Arbabi, Y. Horie, M. Bagheri, and A. Faraon, Nat. Nanotechnol. **10**, 937 (2015).
22. W. T. Chen, P. Török, M. R. Foreman, C. Y. Liao, W. Y. Tsai, P. R. Wu, and D. P. Tsai, Nanotechnology **27**, 224002 (2016).
23. N. A. Rubin, A. Zaidi, M. Juhl, R. P. Li, J. P. Balthasar Mueller, R. C. Devlin, K. Leósson, and F. Capasso, Opt. Express **26**, 21455 (2018).
24. D. D. Wen, F. Y. Yue, G. X. Li, G. X. Zheng, K. L. Chan, S. M. Chen, M. Chen, K. F. Li, P. W. H. Wong, K. W. Cheah, E. Y. B. Pun, S. Zhang, and X. Z. Chen, Nat. Commun. **6**, 8241 (2015).
25. F. Y. Yue, X. F. Zang, D. D. Wen, Z. I. Li, C. M. Zhang, H. G. Liu, B. D. Gerardot, W. Wang, G. X. Zheng, and X. Z. Chen, Sci. Rep. **7**, 11440 (2017).
26. P. Yu, J. X. Li, C. C. Tang, H. Cheng, Z. C. Liu, Z. C. Li, Z. Liu, C. Z. Gu, J. J. Li, S. Q. Chen, and J. G. Tian, Light Sci. Appl. **5**, e16096 (2016).
27. Z. C. Li, W. W. Liu, H. Cheng, S. Q. Chen, and J. G. Tian, Sci. Rep. **5**, 18106 (2015).